Nuclear Engineering and Technology 51 (2019) 1860–1865

Contents lists available at ScienceDirect

Nuclear Engineering and Technology

journal homepage: www.elsevier.com/locate/net

Technical Note

Measurement of fast ion life time using neutron diagnostics and its application to the fast ion instability at ELM suppressed KSTAR plasma by RMP

Jong-Gu Kwak*, M.H. Woo, T. Rhee

National Fusion Research Institute, Daejeon, 305-333, South Korea

ARTICLE INFO

Article history:
Received 22 October 2018
Received in revised form
29 January 2019
Accepted 19 May 2019
Available online 20 May 2019

Keywords:
KSTAR
neutron
fast ion

ABSTRACT

The confinement degradation of the energetic particles during RMP would be a key issue in success of realizing the successful energy production using fusion plasma, because a 3.5 MeV energetic alpha particle should be able to sustain the burning plasma after the ignition. As KSTAR recent results indicate the generation of high-performance plasma(β_p~3), the confinement of the energetic particles is also an important key aspect in neutral beam driven plasma. In general, the measured absolute value of the neutron intensity is generally used for to estimating the confinement time of energetic particles by comparing it with the theoretical value based on transport calculations. However, the availability of, but for its calculation process, many accurate diagnostic data of plasma parameters such as thermal and incident fast ion density, are essential to the calculation process. In this paper, the time evolution of the neutron signal from an He3 counter during the beam blank has permitted to facilitate the estimation of the slowing down time of energetic particles and the method is applied to investigate the fast ion effect on ELM suppressed KSTAR plasma which is heated by high energy deuterium neutral beams.

ELM(Edge Localized Mode) suppression is known to be one of key issues in ITER and near-future fusion reactors because the diverter heat exceeds the present engineering limit during the ELM transient period. Several suppression methods have been proposed, but the most promising approach involves the application of a 3D RMP(Resonant Magnetic-field Perturbation) field to the boundary area of the plasma volume [1]. It is also well known that degradation of thermal ions and electron confinement occur during the application of the RMP. However, there are limited studies on the confinement of energetic particles.

Contrary to present research on medium size tokamaks, it is expected that fast ion confinement, including alpha particle confinement could be a major issue when RMP is applied to the burning plasma state in ITER and other fusion reactors. As such, particle confinement in the case of ELM suppression and the application of RMP is a research topic of significant interest. KSTAR has produced excellent results on ELM suppression, particularly with regard to sustaining long pulse periods by applying perturbative magnetic fields of low toroidal mode number [2]. During the ELM suppression period by RMP, we note the fishbone (FB) activity and mode amplitude of FB decreased with an increase of the RMP intensity, but the energetic particle confinement is enhanced. The main objective of the Korea Superconducting Tokamak Advanced Research (KSTAR) program is the exploration of the underlying physics and associated technologies related to the high-performance steady state of a tokamak that are essential to the operation of a fusion reactor. As such, its performance has been extended over the current tokamak operation boundary year by year, and recent results indicate the generation of high-performance plasma (β_p~3). In addition, the confinement of energetic particles is also an important aspect in the overall confinement in the case of neutral beam driven plasma in the KSTAR.

There are several direct diagnostic methods for evaluating the fast ion transport behavior, including the FILD (Fast ion loss detector), neutral particle analyzer (NPA), and FIDA(Fast-Ion D-alpha). However, they each require significant effort to deduce the confinement time from the raw experimental data. As a result, indirect methods such as neutron measurement are generally used to analyze fast ion behavior because neutron production is proportional to the fast ion intensity in beam driven plasma, [3–6]. However, neutron emission is a complicated function of many

* Corresponding author.
E-mail address: jgkwak@nfri.re.kr (J.-G. Kwak).

https://doi.org/10.1016/j.net.2019.05.016

plasma parameters. In particular, the Zeff (Effective Z number) is an important parameter in estimating thermal ion density. It is necessary to establish an accurate information of the plasma profile in advance of estimating slowing down time measurement. As such, the fast time response of the signal is used instead of the absolute value and a scintillator detector is generally utilized to determine the time response of neutron signals due to their fast time response. However, the scintillator detector has a drawback of the gamma discrimination. Alternatively, a convention proportional counter using He3 filled or FC (fission counter) facilitates more accurate gamma discrimination but encounters difficulty during pulse shaping at high speeds. In this paper, we applied the He3 and FC for fast response neutron measurements with a field programmable gate array (FPGA), and a fast digital signal processor (DSP), with a good time resolution to the time response of the neutron signal [7]. In addition, the decay time of the beam blank period is used, where the blank beam time should be performed for CES(Charge Exchange Spectroscopy), and MSE(Motional Stark Emission) for background noise subtraction. Fig. 1 shows top view of KSTAR with NBI and diagnostic system.

The neutron decay time at the beam heated plasma is given in many textbooks as [5,8];

$$\tau_n = \frac{\tau_e}{3}\ln\left(\frac{E_b^{1.5}+E_c^{1.5}}{E_n^{1.5}+E_c^{1.5}}\right) \quad (1)$$

where τ_e is the slowing-down time of the electrons, and E_n is the energy at which the fusion reactivity decreases to e^{-1} of its value at E_b. It is nominally set to zero. So by comparing the calculated slowing down time τ_n with the measured one τ_{mn}, the difference $\tau_n - \tau_{mn}$ or the ratio, $1-\tau_{mn}/\tau_n$ corresponds to the addition abnormal MHD activity.

Fig. 2 shows diagrammatic representations of both the conventional and modified new method. In the conventional method, a very short pulse of a neutral beam is injected into the target plasma, and the decay time of the neutron signal is used to estimate the slowing down time of energetic particles. In these cases of the new method, the decay time during the blank beam period is used (gray area in Fig. 2(b)), even though slowing down time is a little bit overestimated due to existing beam ion. Since the blank beam is generally used for other diagnostic purposes, it can be combined with other beam diagnostics to satisfy the requirement of a high-speed linear response neutron detector for slowing down time measurement. The beam blank is used for CES (charge exchange spectroscopy) measurements at normal operation or naturally occurs during the fault mode of the NBI beam. A nominal blank period of a beam for diagnostic purposes is about 10 msec, and the retrigger time for the NBI interlock is set to 10–20 msec. Therefore, the plasma parameters do not change very much during the blank period, and this facilitates measurement of the slowing down time. In general, the central electron temperature and stored energy decrease by less than 10%. The feasibility test of a new method is done on shot # 18483 as shown in Fig. 3, where the ITB(Internal Transport Barrier), L and H-mode are formed a single shot. Firstly, ITB is formed at inboard limited plasma and the ion temperature increases up to 6 keV in weakly reverse shear q profile, but it comes back transition to L-mode. It also transitioned to H-mode around 5.8s with detaching from the inboard limiter to diverted plasma. Note that during the H-mode(6–7s), broadband MHD activity with a frequency up to 100 kHz was measured as shown in Fig. 3. The beam voltage of each ion source was 100 keV, 65 keV and 95 keV. The ratio of the measured to theoretical slowing down time is about 80–90% in the L-mode and drops to 50% in the H-mode as shown in (e). When the spectogram of MC(Mirnov Coil) shown in Fig. 3(b) is

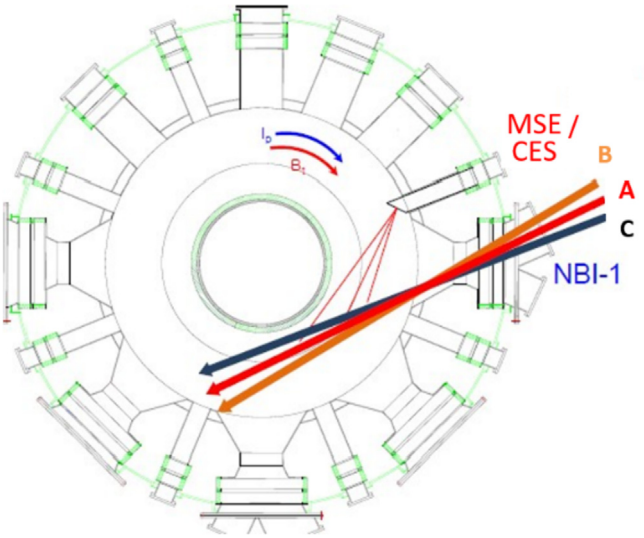

Fig. 1. Schematic view of NBI and diagnostic system in KSTAR.

examined, a significant increase in the amplitude for toroidal mode numbers of 1 and 2 is observed. It is located at q < 2 based on the ECE(Electron Cyclotron Emission) spectrogram signal. Another interesting observation is that during the interval ranging from 3 to 6 s(L-mode), the mode amplitude decrease corresponds to an

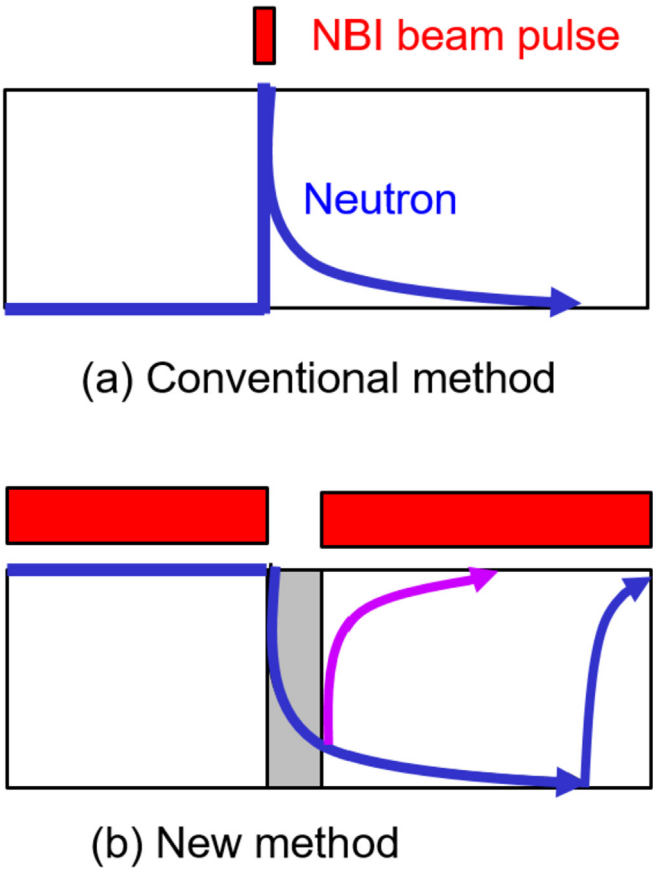

Fig. 2. Schematic diagram of neutron decay time measurement. (a) Conventional method. (b) New method. The beam pulse is represented as a red block and the neutron signal as blue and purple arrows. The shaded region represents the diagnostic area of the new method during beam blank. (For interpretation of the references to colour in this figure legend, the reader is referred to the web version of this article.)

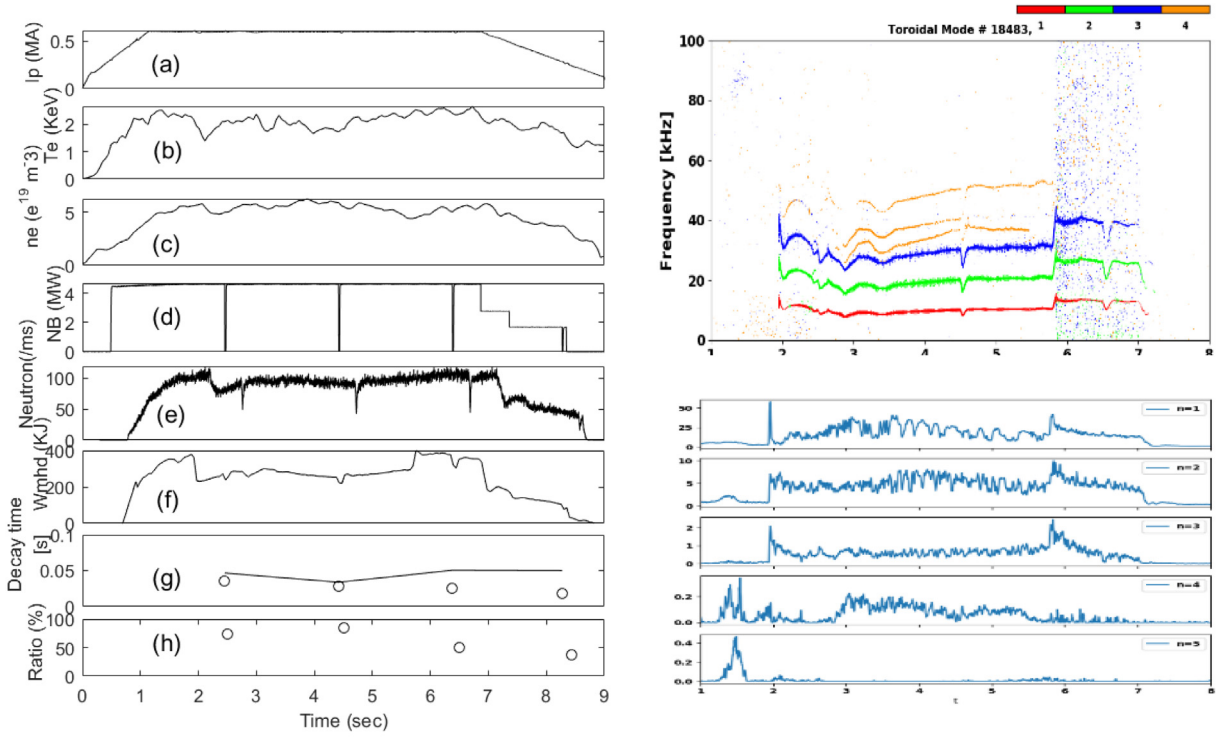

Fig. 3. Time evolution of the plasma discharge of shot #18483: (a) plasma current (b) electron temperature, (c) plasma density, (d) neutral beam power, (e) neutron flux (f) stored energy, (g) slowing down time (solid line represents calculated values), (h) τ_{mn}/τ_n, where three beam blank are used at 2.5, 4.5, 6.5 s and [b] spectrogram and integrated mode amplitude from Mirnov coil.

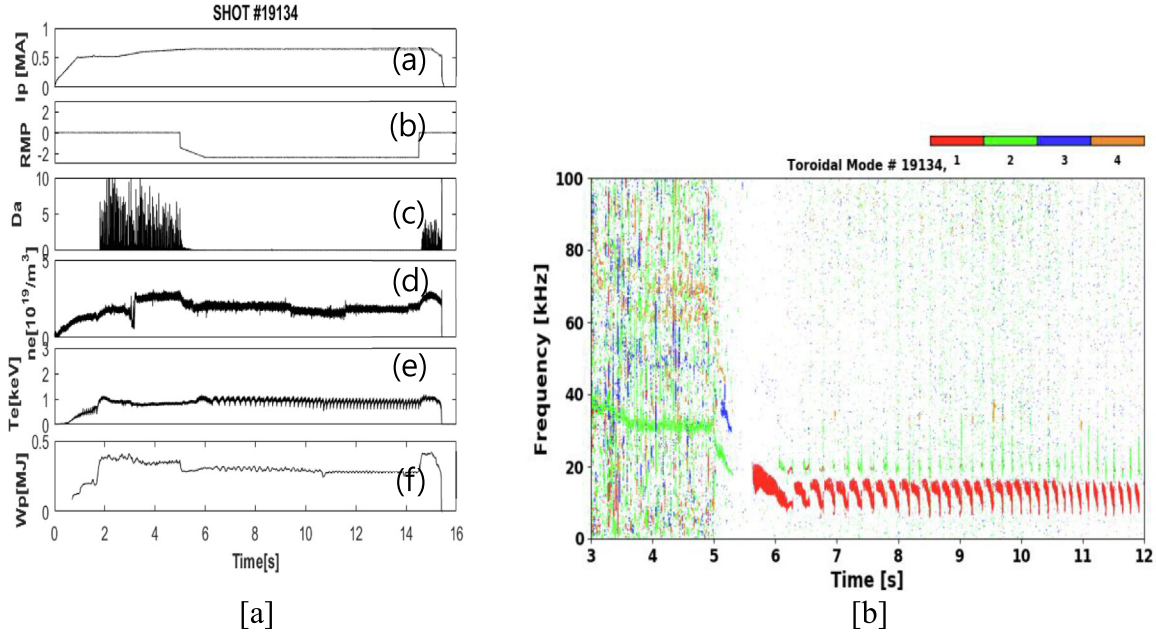

Fig. 4. Time evolution of the plasma discharge of shot #19134[a]: (a) plasma current (b) RMP amplitude, (c) D-α signal, (d) electron density, (e) electron temperature, (f) stored energy. [b] spectrogram from Mirnov coils showing the MHD activity and from 5.5s, strong fish bone activity is observed during ELM suppressed period by RMP.

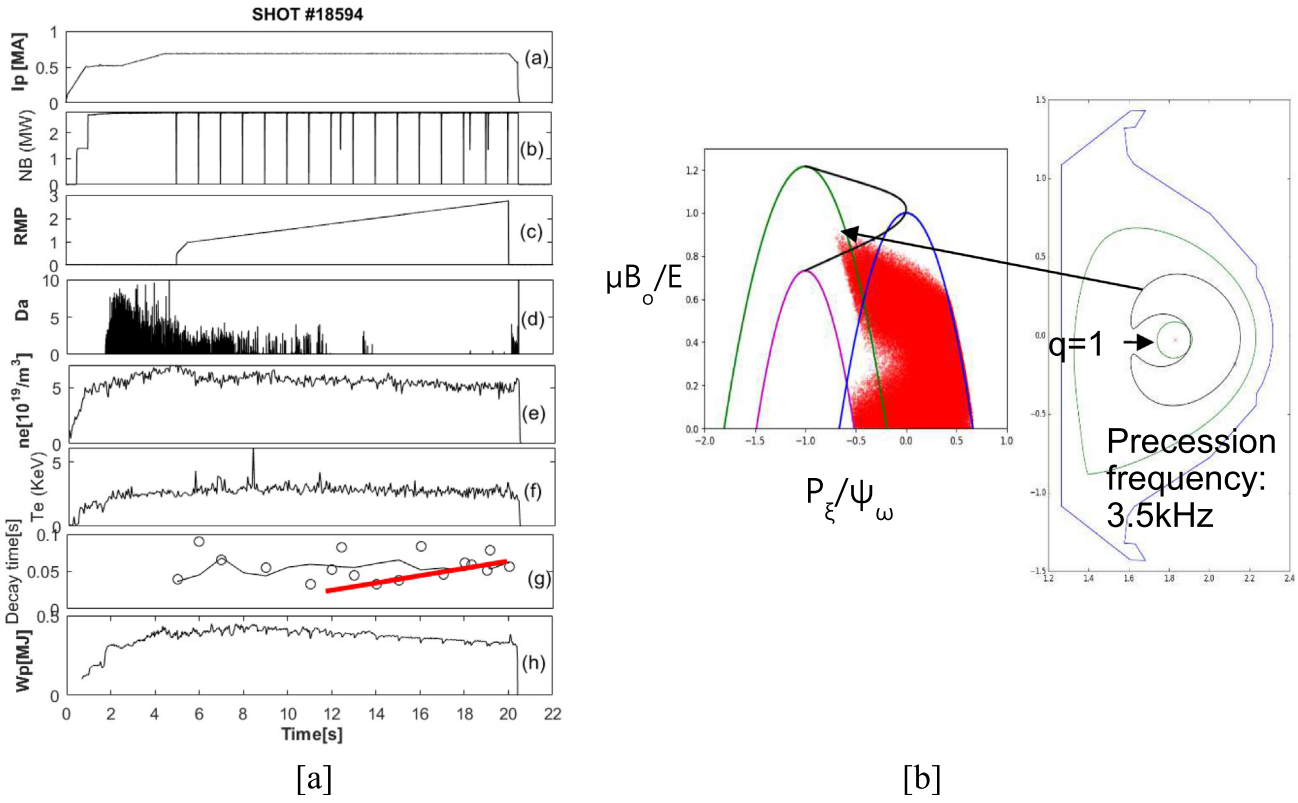

Fig. 5. Time evolution of the plasma discharge of shot #18594[a]: (a) plasma current, (b) neutral beam power, (c) amplitude of RMP, (d) D-a, (e) electron density, (f) electron temperature, (g) calculated (solid line) and measured slowing down time(black circle) (h) stored energy. [b] orbit analysis shows that some particles are located in the trapped region and their trajectory is located on q = 1 surface.

increase of the neutron signal. However, no significant change is observed in the slowing down time from the neutron signal. Therefore, in order to evaluate the beam transport loss in relation to the MHD mode activity, two separate evidence should be considered. The first one is the change of the slowing down time and the second one is the corresponding mode amplitude change.

KSTAR has demonstrated excellent ELM suppression using n = 1, or n = 2, or combination of both. The #19134 shows a typical ELM suppression discharge using n = 2 RMP where q95 is approximately 4 and the toroidal phase is 90°. It is interesting to note that as soon as RMP is applied, the fishbone-like MHD activity is appeared and is maintained during RMP as shown in Fig. 4(b). The chirp frequency is also observed at interferometer fluctuations signal. ELM is suppressed at approximately 5 s as soon as the RMP is applied.

This is similar to the recent observation in DIII-D that during ELM suppressed fully non-inductive hybrid discharge, benign fishbone-like oscillation appeared during ECCD(Electron Cyclotron Current Drive) replacing previous Alfven eigenmode activity and reducing anomalous beam ion diffusion by a factor of 2 [9]. As shown in Fig. 4(b), maximum frequency of the fishbone is found to be 17 kHz with chirping frequency about 7 kHz. The frequency of fishbone keeps 17 kHz where it started for 1 ms while mode amplitude grows and saturate. Then for the next 1–1.5 ms mode amplitude decreases together with chirping down of the frequency to the plasma rotation frequency. It has been found that q = 1 surface is about r = 15 cm and CES observation indicates that toroidal rotation frequency is about 10 kHz. In other words, fishbone frequency at plasma-rest frame is about 7 kHz. This observation is a little different with result from ASDEX-U where fishbone mode has maximum amplitude when frequency is chirped down to rotation frequency and then mode gradually disappears [10].

It is widely accepted that this activity has two possible origins. One is the excitation through the resonant interaction of a fast-ion population in the plasma with the kink mode near the q = 1 surface [11]. The other one is inclusion of the diamagnetic effect of ions that ion-viscosity related momentum transfer drives the mode [12–14]. If we assume that fishbone mode we observed is driven unstable through resonant hot particle – kink mode interaction, Krass.et al. has shown that to access fishbone unstable region, either density, or core electron temperature should be increased in order that hot particle beta can excess critical beta for destabilization. But one can see that from Fig. 5, plasma density reduced while core Te remains constant during the RMP injection. Clearly this is not our case and we can guess that our fishbone mode is probably not energetic particle-driven mode. To understand this point more clearly, we analyzed hot particle trajectory in more detail using test particle trajectory simulation.

Fig. 5(b) shows the beam trajectory of barely trapped and passing beam using orbit code(NuBDeC) and small number of particle is located in the trapped region and is overlapped with q = 1 surface [15]. To check existence of trapped particles deposited

Table 1
The thermal and fast ion components for various RMP amplitudes. The calculation is done by TRANSP using profile data as shown in Fig. 6.

Time(sec)	6.8	12.2	18.7
RMP(kA/t.)	1	1.6	2.3
Wmhd(kJ)	385	360	316
F_thermal(%)	53	50	47
F_fast(%)	47	50	52

by NBI, we introduce the momentum phase space analysis of beam ions. The three-dimensional orbit is projected to a two-dimensional space for the conserved momentum on axisymmetric system: the canonical toroidal angular momentum and magnetic momentum. With single-energy ions, a geometrical point can be illustrated as a group of momentums. Particles passing the point on the line of a given an arbitrary R position (fixed Z position of magnetic axis) form a hyperbolic line and it is shown on the left of Fig. 5(b). Each line means high/low field side plasma boundary passing(purple/green respectively), magnetic axis passing (blue), and maximum value of hyperbolic lines (black). Thus, trapped particles are represented by the area surrounded by black line because particle can only passing low field side not high field side. Deposited fast ions by NBI1-A with 100 keV energy is projected on the phase space as red dots on the left of Fig. 5(b). We test a trapped particle whether it crosses the q = 1 surface or not. Only barely trapped particles orbit (black banana line) pass through the q = 1 surface presented by the inner green line in the right of Fig. 5(b). Its precession frequency is 3.5 kHz which is half of the measured fishbone frequency. Deeper trapped particles does not pass the q = 1 surface. The other beam source NBI1−B does not generate trapped ions too. Single particle trajectory calculation also shows fast particles due to NBI does not have enough trapped particle fraction to drive fishbone and characteristic frequency of barely trapped particle does not match to the experimental observation. More importantly, when RMP is applied, fast particle loss would increase and hot particle beta would decrease, which is unfavorable for fishbone drive. Effect of RMP on fast particle would be discussed in detail in the next paragraph. All these evidences indicate that our fishbone is ion-diamagnetic type. Following Coppi et al., fishbone frequency of the diamagnetic branch is given approximately as

$$\omega_{*i} = \frac{ck_\theta}{eBn}\frac{dp_{i\perp}}{dr} \tag{2}$$

Assuming pressure as p = nkT, with kinetically reconstructed EFIT(Equilibrium FIT), we can calculate pressure gradient. Setting R(q95) = 15 cm, n = 2.9*10^{19}/cm^3, diamagnetic frequency or fishbone frequency is found to be about 7.8 kHz which is in well match with experiment observation. Also, during RMP, plasma βp has been increased which is key-point for destabilization of diamagnetic type fishbone instability. Even though there is no explicit evidence that this is ion diamagnetic branch fishbone, detailed understanding on fast particles reveals ion-diamagnetic nature of the fishbone instability.

To investigate the dependence of the RMP amplitude on the fast ion behavior, the former is increased from 1 kA/t to 3 kA/t in #18594, where the RMP is applied from 5 s onwards and the field intensity is increased as shown in Fig. 5(a)(c). Before ELM suppression, τ_{mn} does not change and is independent of the RMP amplitude. However, after ELM suppression at approximately 12 s, τ_{mn} increases and $\tau_n - \tau_{mn}$ decreases with RMP. The global τ_{mn} is proportional to RMP, but the local fast ion loss may be related to the island structure around the pedestal and the direction in which the RMP is applied. Mode amplitude of n = 1 also decreased during ELM suppression period as shown in Fig. 7. When we compare the result of fast ion fraction at 12.2 s with 18.7 s, it is seen that the fraction of the fast ion component is increased as shown in Table 1, and $\tau_n - \tau_{mn}$ (corresponds to abnormal beam diffusion) decreases. The calculated ion diamagnetic frequency based on the plasma profile as shown in Fig. 6 is about 8 kHz and the measured frequency is about a few kHz so that measured fish bone activity is between ion diamagnetic and barely trapped particle frequency as in reference 12. Note that deviated measured decay constant values around 6, 12, 19s in Fig. 5(g) could be omitted from analysis because

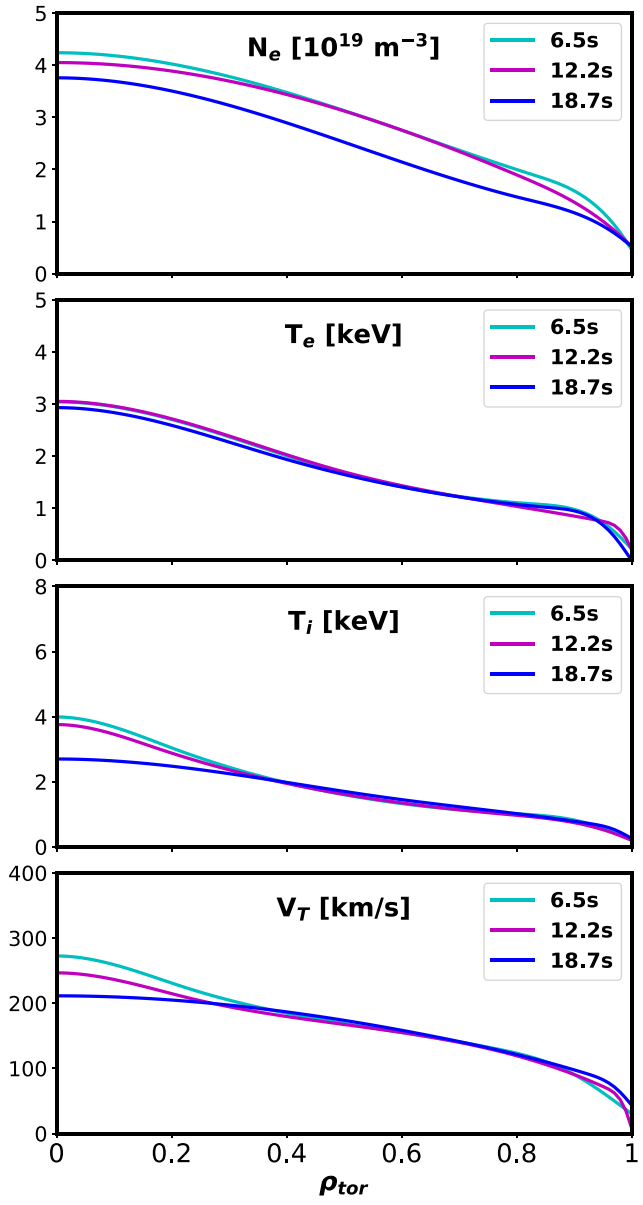

Fig. 6. Plasma profiles for RMP ELM-suppressed discharge for different RMP amplitudes.

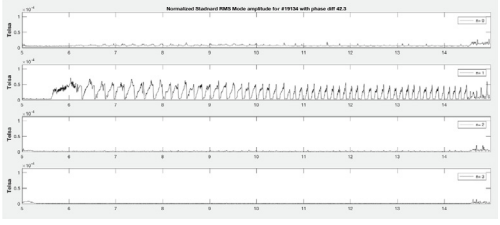

Fig. 7. Mode amplitude measured by Mirnov coils.

they are on ELM event or one beam source is on.

In summary, an experiment to measure the slowing down time of fast ions in beam driven KSTAR plasmas was performed for various discharge cases using new method in neutron diagnostics. These measurements were performed during the beam blip time for plasma diagnostics based on a pulse mode He3 neutron counter.

The feasibility study demonstrated that the blank beam method could be useful for estimating the slowing down time of fast ions in KSTAR. For example, the measured slowing down time for the ITB and L-mode is nearly the same as the calculated value. Moreover, the measured slowing down time is less than the theoretical one for the H-mode, and this is likely due to MHD activity. During the ELM suppression period due to RMP, fishbone (FB) activity with the frequency of a few kHz was observed. The FB mode amplitude decreased and corresponding MHD activity measured by neutron diagnostics is also decreased with the RMP intensity.

Acknowledgement

This work was supported by the KSTAR research project funded by the Minister of Science and ICT of Korea and one of authors (J.G. Kwak) thanks to J.S. Kang for his profile data managements.

References

[1] A. Loarte, G. Huijsmans, S. Futatani, L.R. Baylor, T.E. Evans, D.M. Orlov, O. Schmitz, M. Becoulet, P. Cahyna, Y. Gribov, et al., Nucl. Fusion 54 (2014), 033007.
[2] Y. In, J.K. Park, J.M. Jeon, J. Kim, M. Okabayashi, Nucl. Fusion 55 (4) (2015), 043004.
[3] J.D. Strachan, P.L. Colestock, S.L. Davis, D. Eames, P.C. Efthimion, H.P. Eubank, R.L. Goldston, L.R. Grisham, R.L. Hawryluk, J.C. Hosea, et al., Nucl. Fusion 21 (1981) 67.
[4] M. Isobe, M. Sasao, S. Okamura, T. Kondo, S. Murakami, T. Minami, S. Kado, K. Ida, A. Shimizu, M. Osakabe, et al., Nucl. Fusion 41 (2001) 1273.
[5] W.W. Heidbrink, Jinchoon Kim, R.J. Groebner, Nucl. Fusion 28 (10) (1988) 1897.
[6] W.W. Heidbrink, J.R. Ferron, C.T. Holcomb, M.A. Van Zeeland, Xi Chen, C.M. Collins, A. Garofalo, X. Gong, B.A. Grierson, M. Podesta, et al., Nucl. Fusion 56 (2014) 195030.
[7] J.G. Kwak, H.S. Kim, M.S. Cheon, S.T. Oh, Y.S. Lee, Fusion Eng. Des. 109–111 (A) (2016) 608.
[8] J. Wesson, Tokamaks, Oxford University Press, 2011, p. 249.
[9] C.C. Petty, R. Nazikian, J.M. Park, F. Turco, Xi Chen, L. Cui, T.E. Evans, N.M. Ferraro, J.R. Ferron, A.M. Garofalo, et al., Nucl. Fusion 57 (2017) 116057.
[10] T. Kass, H.-S. Bosch, F. Hoenen, K. Lackner, M. Maraschek, H. Zohm, Nucl. Fusion 38 (1998) 807.
[11] L. Chen, R.B. White, M.N. Rosenbluth, PRL 52 (1984) 1122.
[12] B. Coppi, F. Porcelli, PRL 57 (1986) 2272.
[13] B. Coppi, B. Migiuolo, F. Porcelli, Phys. Fluids 31 (1988) 1630.
[14] W.W. Heidbrink, G. Sager, Nucl. Fusion 30 (1990) 1015.
[15] T. Rhee, 12th Japan-Korea Workshop on "Modeling and Simulation of Magnetic Fusion Plasmas", Inuyama International Sight Seeing Center (FREUDE), Japan, 2017.